Contents list available at IJRED website

Int. Journal of Renewable Energy Development (IJRED)

Journal homepage: http://ejournal.undip.ac.id/index.php/ijred

Research Article

Application of Response Surface Methodology to Predict the Optimized Input Quantities of Parabolic Trough Concentrator

Vijayan Gopalsamy[a*], Ramalingam Senthil[b], Muthukrishnan Varatharajulu[c], Rajasekaran Karunakaran[d]

[a]*Department of Mechanical Engineering, KSK College of Engineering and Technology, Tamilnadu, India*

[b]*Department of Mechanical Engineering, SRM Institute of Science and Technology,Kattankulathur,Chennai, India*

[c]*Department of Mechanical Engineering, National Institute of Technology-Trichy, Tamilnadu, India*

[d]*Department of Mechanical Engineering, Anna University, Chennai, Tamilnadu, India*

ABSTRACT. This work carries out a numerical investigation on aluminium oxide/de-ionized water nanofluid based shield-free parabolic trough solar collector (PTSC) system to evaluate, validate, and optimize the experimental output data. A numerical model is developed using response surface methodology (RSM) for evaluation (identifying influencing parameters and its level) and single objective approach (SOA) technique of desirability function analysis (DFA) for optimization. The experimental data ensured that global efficiency was enhanced from 61.8% to 67.0% for an increased mass flow rate from 0.02 kg/s to 0.06 kg/s, respectively. The overall deviation between experimental and numerical is only 0.352%. The energy and exergy error was varied from 3.0% to 6.0%, and the uncertainty of the experiment is 3.1%. Based on the desirability function analysis, the maximum and minimum efficiencies are 49.7% and 84.9%, as per the SOA technique. This numerical model explores the way to enhance global efficiency by 26.72%.

Keywords: Parabolic trough solar collector, nanofluid, optimization, response surface methodology, shield-free receiver.

Article History: Received: 14th May 2020; Revised: 29th June 2020; Accepted: 5th July 2020; Available online: 8th July 2020

How to Cite This Article: Vijayan, G., Senthil, R., Varatharajulu, M. and Karunakaran,R. (2020) Application of Response Surface Methodology to Predict the Optimized Input Quantities of Parabolic Trough Concentrator. *International Journal of Renewable Energy Development*, 9(3), 393-400

https://doi.org/10.14710/ijred.2020.30092

1. Introduction

Solar energy is coming under the category of renewable sources of energy like others sources, such as wind, geothermal, biomass, and ocean energy. Still, the unique features of solar energy like reliability, accessibility, and low-cost energy acquiring technology make it always in limelight status. All these points support solar energy to adopt in various kinds of domestic and industrial applications (Farshad and Sheikholeslami, 2019). A solar thermal collector is one of the vital modes, to absorb and convert the radiation into thermal energy (Rahmati and Niazi, 2015). The design of solar collectors, receiver, and other techniques were developed already (Moradikazerouni *et al.* 2019). Application of graphite nanoparticles in a direct absorption solar collector (DASC) and the use of alumina-water nanofluid for improving heat absorption capability was studied (Senthil and Cheralathan, 2016; Senthil, 2019). Parabolic dish (Senthil and Cheralathan, 2019) and parabolic trough solar collector (PTSC) are the most matured technology (Vijayan and Karunakaran, 2019), in which phase change material (PCM) and nanofluid proved the enhanced performance experimentally. Mohsen and Mostafa (2018) used water, Al_2O_3/water nanofluid, and CuO/water nanofluid as heat transfer fluid (HTF) in flat plate solar collectors. They studied the performance analytically using an artificial neural network tool and ensured less than ±2% deviation. Vijayan *et al.* (2019) experimentally analyzed the effect on performing aqueous alumina-based unshielded absorber type PTSC in outdoor conditions. Reza *et al.* (2019) reviewed the efficiency enhancement techniques such as using nanofluid as HTF, design parameter, performance factor, economic factor, and comparison of results.

Sami (2018) developed a numerical model to explore the possibilities of maximizing the thermal performance of solar collectors. Shrikant *et al.* (2018) investigated the adaptability of multivariate non-linear analysis and grey wolf optimization techniques in PTSC integrated concentrating solar thermal power. Tahereh and Ranjbar (2017) experimentally analyzed the influence of running conditions on the performance of nanofluid based DASC. Response surface methodology (RSM) used to identify the

*Corresponding author: viji_laker@yahoo.co.in

optimized response values such as energy and exergy efficiencies of magnetite, graphite, and silver. About 11.26% and 87.39% are exergy and energy efficiency observed by Jiangfeng and Xiulan, (2016). Anissa, Hatem, and Philippe (2015) carried out the numerical analysis to optimize the PTSC receiver tube using SolTrace and computational fluid dynamics (CFD) software. Amin and Mehran (2020) investigated the optimized effect of mirror configuration on the linear Fresnel concentrator's energy and exergy performance. Majedul *et al.* (2012) developed the model to optimize both optically and thermally using the monte carlo ray tracing method (MCRT), and observed the maximum and mean relative error between simulation and experimental result as 2.95% and 1.70% (Dudley *et al* 1994); 5.09% and 1.82% (Cheng *et al.* 2010). Mohamed (2014) analyzed the receiver's spectral radiation characteristics, PTSC concentrator surface using the MCRT and finite element method.

Saman *et al.* (2017) used RSM to optimize the geometry of cascade solar still and proved 22% productivity enhancement for increased nanoparticle concentrations from 0 to 5%. Venkata and Hameer (2019) carried out the multi-objective optimization technique on solar-based heat engines to establish performance enhancement. Tahereh and Ranjbar (2015) investigated the optimized geometry for thermal efficiency enhancement of nanofluid-based DASC. Hatami and Jing (2017) proposed the best-curved profile of PTSC with the help of RSM. Sarafraz *et al.* (2019) developed RSM based model to optimize the operating parameters and enhance the efficiency of the thermosyphon heat pipe integrated evacuated tube solar collector. Carrying out of experimental work is a time-consuming activity and also to be monitored physically for a definite period. Various techniques such as genetic algorithms (GA), particle swarm optimization (PSO) and RSM are available to optimize the parameters, reducing the experimental work and cost. Alireza and Askarzadeh (2016) discussed the performance of different optimization techniques such as GA and PSO on solar and wind energy, to solve the optimization issues and thermodynamics parameters (energy and exergy). The PTSC system was modeled using a dynamic tool and checked its effectiveness using GA (Risi *et al.* 2013; Bruno *et al.* 2014; Cabello *et al.* 2011). Ze-Dong *et al.* (2015) applied the PSO-MCRT technique to optimize the optical performance of PTSC. Runtime reduction method improved computational time and reduced cost, which explored good agreement with experimental data by Cheng *et al.* (2014).

The literature ensured that good quantity of research work on optimization in terms of profile geometry, optical, and thermal with the help of various optimization techniques such as GA, PSO, and grey analysis on various solar collectors was carried out. They used mostly RSM based optimization on DASC. A minimal work was done on PTSC using RSM. There were very few works available on parameter optimization of PTSC. Hence, the present work investigates the influence of factors, influencing levels, deviation from experimental results, reliability, and consistency of the mathematical model. The optimized values of input parameters derived from the present model such as ambient temperature, beam radiation, Re, Nu, thermal conductivity, specific heat, heat removal factor, and heat transfer coefficient of alumina/DIW nanofluid based PTSC are reported here.

2. Materials and Methods

2.1 Experimental work

The PTSC experimental platform was tested for various nanofluid concentrations ($0 \geq \phi \leq 4.0\%$) and mass flow rate ($0.02 \geq \dot{m} \leq 0.06$kg/s) to investigate global efficiency. Each concentration (nine concentrations) was tested for all the five mass flow rates. Alumina/DI water nanofluid was stored in HTF tank and pumped through receiver and heat exchanger by mini submersible pump. The performance parameters of PTSC are discussed as follows. Efficiency of PTSC is the ratio of heat absorbed by fluid to the solar radiation fall on the aperture of the collector by Eq. (1) and the exergy efficiency by Patela's (Patela, 2003) Eq.(2).

$$\eta = \frac{\dot{m} C_p (T_o - T_i)}{A_c G_b} \tag{1}$$

$$\eta_{ex} = \left[\frac{\dot{m}\left[C_p (T_o - T_i) - T_a \ln \frac{T_o}{T_i} \right]}{A_c G_b \left[1 - \frac{4}{3}\frac{T_a}{T_{sun}} + \left(\frac{T_a}{T_{sun}} \right)^4 \right]} \right] \tag{2}$$

Where,

η is the energy efficiency,
η_{ex} is the exergy efficiency,
$\dot{m}$ is the flow rate of HTF,
C_p is the specific heat of HTF,
T_i is the inlet temperature of HTF,
T_o is the outlet temperature of HTF,
T_a is the ambient temperature
T_{Sun} is the Sun's surface temperature (5762 K),
A_C is the aperture area,
G_b is the beam solar radiation.

The wind velocity (Anemometer: ±1 m/s), solar radiation (Solar power meter: ±10 W/m^2), flow rate (Rotameter: 1.0%) and temperature of nanofluid, ambient and surface (Thermocouple: ±0.1°C) are recorded at constant time gap. An uncertainty analysis was made as per the procedure (Kline and McClintock, 1953; Moffat,1988), to validate the experimental measurements. Eq. (3) is used to determine the overall uncertainty of the experiment.

$$\Delta Y = \sqrt{\sum \left(\frac{\delta Y}{\delta X_i} \Delta X_i \right)^2} \tag{3}$$

Where,

Y is the overall uncertainty of the experiment,
ΔXi is the uncertainty of measured quantity, and
ΔYi is the uncertainty of derived quantity.

For the predefined fluid flow rate, the experimental error of global efficiency and exergy efficiency varied between 3.0-6.0% for the selected flow rate and concentrations. Overall uncertainty was calculated as 3.1%. Parametric measurements are followed as per the ASHRAE standards 93-2010, which ensures the stability of experiments.

2.2 Analytical description

Various optimization techniques and methods are used to predict the thermal performance as well as experimental design. Many researchers carried out optimization work with different views, other than input parameters so far.

Table1
Status of factors and response

Factors	Low (-1)	High (+1)
A - Ambient Temperature	32.20	37.500
B - Solar Radiation	485.0	876.00
C- Reynolds number of nanofluid	2150	7551.0
D - Nusselt number of nanofluid	11.11	48.540
E - Thermal conductivity of nanofluid	0.628	0.7781
F - Specific heat of nanofluid	3621	4179.0
G - Heat removal rate	0.987	0.9968
H - Heat transfer coefficient	487.0	1943.0
η_g - Global efficiency	66.00	67.00

Analysis of variance (ANOVA) methodology is used to consolidate the experimental values for their significance on the model coefficient. Here, ANOVA-RSM-Historical design data type is used to validate the experimental work, analyze the influence of input parameter on collector performance and finally to predict the optimized values through single point approach analysis. 45 numbers of experimental runs, 8 numbers of input factors and one number of responses, totally 405 numbers of data are used in this numerical modeling work. By uploading all this data, the summary such as the factors, response, and their levels are generated, which are given in Table 1.

2.1 Model and description

The model detail (Table 2) includes the consequence of the model and influencing status of factors. F-value and P-value are the measures of prominence of the model and the significance of the factors. The "F-value" of 21.00 implies that the proposed model is significant. Here, the ambient temperature, solar radiation, thermal conductivity of nanofluid, and specific heat of nanofluid are considerable model terms due to its F-value (< 0.05). Values greater than 0.1 indicate the model terms are not significant. It does not mean that other factors are not significant; it means the level of influence is low. Fig. 1 represents the statistical value of the model graphically. The performance indicators such as R^2 (coefficient of determination): to ensure the predicted model; Adjusted R^2: to compare the residual per unit degree of freedom; Adequate precision (≥ 4.0): to explore the influence of control free factors over the response.

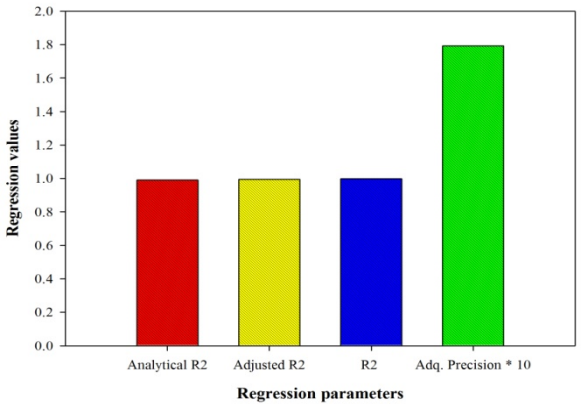

Fig. 1 Statistical quantities

Table 2
Status of model and factors

Factors	Sum of Squares	Mean Square	F-value	p-value Prob. >F	Level of influence
Model	1.733 E-04	2.167 E-05	21.0	<0.0001	Suggested
A	6.900 E-06	6.900 E-06	6.68	0.0140	4
B	1.532 E-05	1.532 E-05	14.8	0.0005	1
C	3.819 E-06	3.819 E-06	3.70	0.0625	5
D	2.622 E-06	2.622 E-06	2.54	0.1199	6
E	8.694 E-06	8.694 E-06	8.41	0.0063	3
F	8.942 E-06	8.942 E-06	8.65	0.0057	2
G	1.630 E-06	1.630 E-06	1.58	0.2172	7
H	1.529 E-06	1.529 E-06	1.48	0.2318	8

Predicted efficiency =

$$0.69405 + (4.72641E-04 \times A) + (7.88738E-6 \times B) - (6.58498E-6 \times C) + (6.20413E-4 \times D) - (0.22704 \times E) - (6.05888E-5 \times F) + (0.34704 \times G) + (9.51058E-6 \times H) \quad (4)$$

Where,
A is the ambient temperature,
B is the solar radiation,
C is the Reynolds number,
D is the Nusselt number,
E is the thermal conductivity of nanofluid,
F is the specific heat,
G is the heat removal factor, and
H is the heat transfer coefficient.

3. Results and Discussion

As per the proposed model, the four input factors, such as ambient temperature, solar radiation, thermal conductivity, and specific heat, influenced on the collector performance. The remaining four factors, such as Re, Nu, heat removal, and heat transfer coefficient, also showed their effect on performance but not as much as the first set of factors. Fig. 2-8 show the effect of factors on global efficiency. It increases along with the increase in ambient temperature and radiation. Due to its linear progress nature, both the ambient temperature (0.0140 < 0.05) and radiation (0.0005 < 0.05), are very sensitive on collector performance. At the same time, an increase in radiation also increases the atmosphere temperature and efficiency. Global efficiency increases with an increase in ambient temperature, but the enhancement is more at low ambient temperature. A decrease in Re had a positive effect on efficiency, as shown in Fig. 3. It has a similar character with instantaneous efficiency and opposite with thermal efficiency. Both the Re (0.0625 > 0.05) and radiation (0.0005 < 0.05) are linear in nature, and Re is not showing much significance like radiation on efficiency. While considering the combined effect of Re (0.0625 > 0.05) and Nu (0.1199 > 0.05), it is similar to instantaneous efficiency (Fig. 4)and has a slightly curved profile nature with thermal efficiency. Fig. 5 shows the influence of Nu (0.1199 > 0.05) and thermal conductivity (0.0063 < 0.05)

on global efficiency. Thermal conductivity has the same type of effect on the Nu, and its decrement enhanced the thermal efficiency sharply. But, both Re and Nu work parallel and linear, where these factors are not significant; that is, they are not influencing much on the performance part. Variation of efficiency, due to effect of thermal conductivity (0.0063 < 0.05) and specific heat (0.0057 < 0.05) is shown in Fig.6. The relation between specific heat (0.0057 < 0.05) and heat removal factor (0.2172 > 0.05) and its influence is shown in Fig. 7. An increase in the heat removal factor leads to an increase in global efficiency, but it was insufficient. Fig. 8 shows that both offered the same type of effects the heat removal factor (0.2172 > 0.05) and the heat transfer coefficient (0.2318 > 0.05) on global efficiency. As per single parameter consideration ambient temperature, solar radiation, Nu, heat removal factor, and heat transfer coefficient were support to enhance the efficiency and Re, thermal conductivity, specific heat were acted in the opposite direction. The combined effect of parameter worked in different ways and changed the quality of influence. The transition range of global efficiency was 66.821-66.232%; below this level, the efficiency was decreased fast and reached to 64.284%. The minimum and maximum efficiency were observed where the thermal conductivity and Nu were 0.6280, 0.3330, and 11.11, 48.54, respectively. Above this level, the model predicts that the efficiency goes towards down.

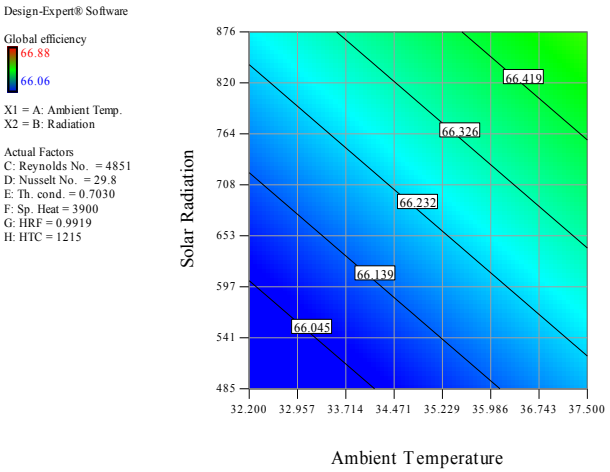

Fig. 2 Effect of ambient temperature and radiation on η_g

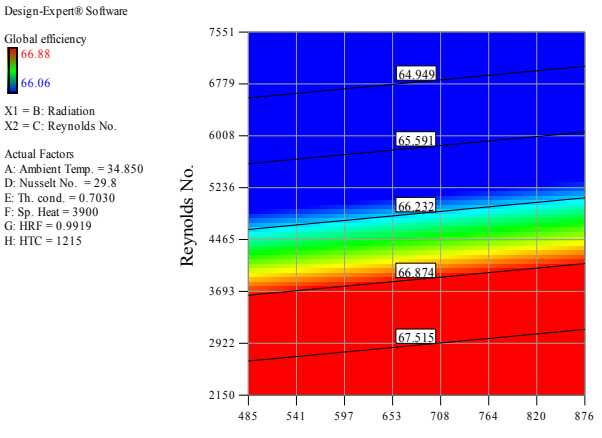

Fig. 3 Effect of radiation and Re on η_g

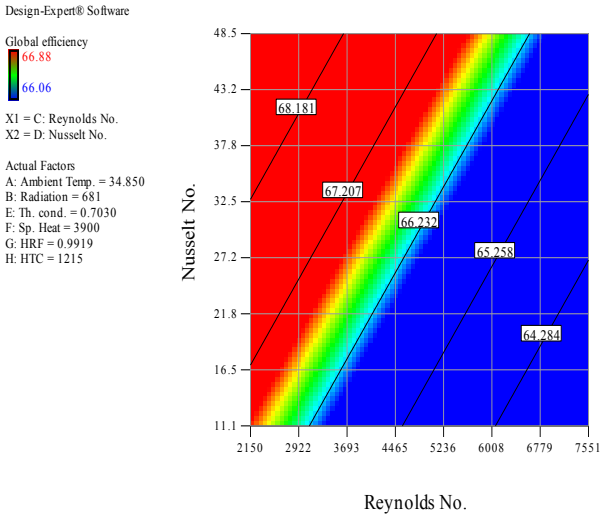

Fig. 4 Influence of Re and Nu on η_g

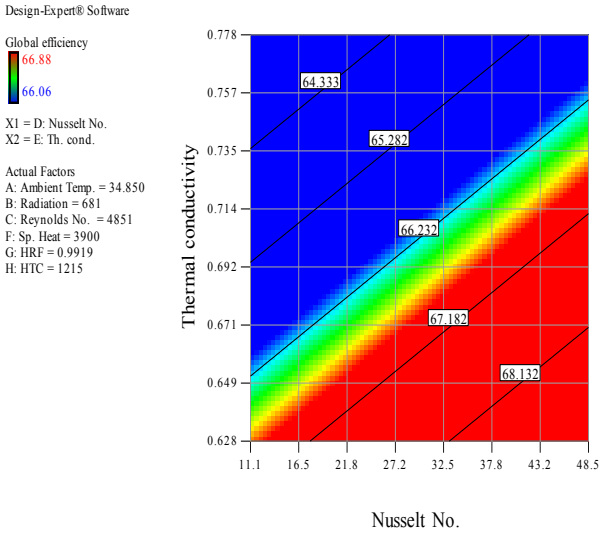

Fig. 5 Influence of Nu and thermal conductivity on η_g

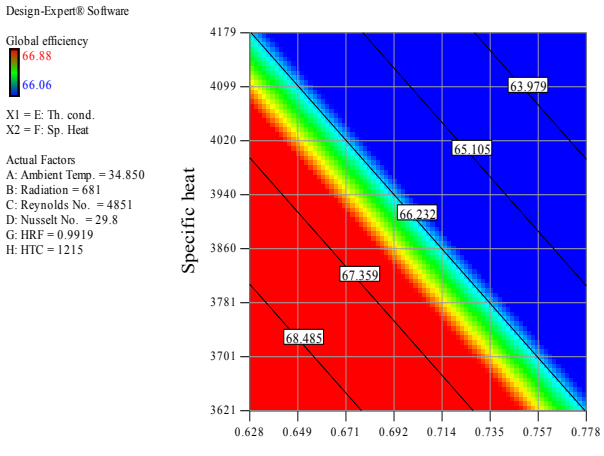

Fig. 6 Effect of thermal conductivity and specific heat on η_g

Table 3
Comparison of experimental and predicted results with factors and response

Run	A	B	C	D	E	F	G	H	Efficiency (Predicted)	Efficiency (Experimental)	Deviation
1	33.80	848	2462	14.34	0.6320	4179.0	0.9880	546	66.08	66.08	0.0031
2	33.40	821	3555	23.28	0.6291	4171.0	0.9925	883	66.42	66.46	0.0657
3	34.20	876	4664	31.63	0.6280	4179.0	0.9943	1197	66.68	66.67	0.0147
4	34.50	873	6019	40.50	0.6302	4178.9	0.9957	1538	66.68	66.66	0.0246
5	33.30	714	7188	48.20	0.6299	4178.8	0.9968	1830	66.47	66.51	0.0642
6	36.50	806	2504	14.29	0.6546	4103.0	0.9884	564	66.12	66.12	0.0000
7	36.00	734	3499	22.57	0.6490	4102.0	0.9927	883	66.53	66.48	0.0693
8	37.50	619	4907	32.15	0.6511	4102.0	0.9947	1261	66.40	66.51	0.1695
9	34.90	485	5953	39.40	0.6511	4102.0	0.9962	1545	66.40	66.37	0.0495
10	37.20	759	7551	48.54	0.6545	4102.0	0.9967	1914	66.54	66.50	0.0634
11	36.10	668	2445	13.75	0.6719	4027.5	0.9888	557	65.94	66.07	0.1964
12	35.90	501	3524	22.39	0.6687	4027.1	0.9936	902	66.42	66.32	0.1451
13	36.50	610	4751	30.91	0.6697	4027.3	0.9951	1247	66.56	66.51	0.0679
14	35.60	568	5999	39.00	0.6704	4027.3	0.9959	1575	66.21	66.44	0.3520
15	36.10	658	7068	46.00	0.6692	4027.2	0.9966	1856	66.70	66.59	0.1687
16	36.70	520	2333	12.87	0.6875	3954.3	0.9893	533	66.29	66.08	0.3106
17	36.70	676	3697	22.82	0.6918	3954.8	0.9936	951	66.31	66.37	0.0941
18	35.50	745	4973	31.30	0.6926	3955.0	0.9952	1306	66.55	66.43	0.1807
19	34.00	690	6033	38.43	0.6903	3954.6	0.9959	1598	66.44	66.42	0.0354
20	35.20	682	7319	46.00	0.6914	3954.7	0.9965	1918	66.57	66.39	0.2715
21	33.80	832	2150	11.56	0.6996	3885.2	0.9870	487	66.26	66.25	0.0109
22	34.70	603	3395	21.00	0.7043	3885.4	0.9928	893	66.40	66.36	0.0602
23	35.20	706	4577	29.13	0.7053	3885.4	0.9947	1238	66.57	66.56	0.0116
24	34.30	648	5738	36.70	0.7056	3885.4	0.9958	1560	66.58	66.52	0.0950
25	35.30	686	7357	45.37	0.7108	3885.7	0.9966	1943	66.13	66.34	0.3144
26	35.00	709	2182	11.51	0.7207	3817.0	0.9872	500	66.18	66.14	0.0578
27	34.30	566	3339	20.42	0.7222	3817.0	0.9929	889	66.19	66.32	0.1972
28	35.50	695	4495	28.18	0.7230	3817.0	0.9947	1228	66.54	66.57	0.0389
29	34.90	703	5663	35.85	0.7235	3817.0	0.9958	1563	66.57	66.60	0.0391
30	34.90	601	6355	41.22	0.7185	3817.0	0.9964	1785	66.77	66.74	0.0471
31	35.30	768	2288	12.00	0.7436	3750.0	0.9879	538	66.03	66.11	0.1204
32	35.80	699	3515	20.93	0.7454	3750.0	0.9931	940	66.18	66.35	0.2519
33	33.10	766	4333	27.23	0.7392	3750.0	0.9947	1213	66.57	66.58	0.0151
34	32.90	758	5567	35.00	0.7413	3749.9	0.9958	1560	66.63	66.55	0.1127
35	32.20	761	6506	41.08	0.7391	3750.0	0.9965	1830	66.54	66.61	0.1105
36	33.70	771	2190	11.26	0.7589	3684.7	0.9874	515	66.07	66.06	0.0092
37	34.30	830	3324	19.74	0.7599	3684.7	0.9925	904	66.44	66.44	0.0037
38	33.90	644	4331	26.85	0.7579	3684.7	0.9947	1226	66.52	66.48	0.0558
39	33.70	537	5107	32.62	0.7534	3684.9	0.9957	1481	66.55	66.61	0.0964
40	34.00	570	6103	38.90	0.7529	3654.0	0.9963	1766	66.76	66.88	0.1776
41	34.30	823	2192	11.11	0.7780	3621.1	0.9871	521	66.10	66.07	0.0459
42	34.10	792	3262	19.07	0.7781	3621.1	0.9923	894	66.35	66.36	0.0120
43	33.70	593	4043	25.18	0.7714	3621.4	0.9946	1171	66.66	66.54	0.1793
44	34.00	685	5264	32.69	0.7744	3621.3	0.9958	1526	66.66	66.60	0.0887
45	34.10	733	6360	39.28	0.7750	3621.1	0.9964	1834	66.72	66.63	0.1320

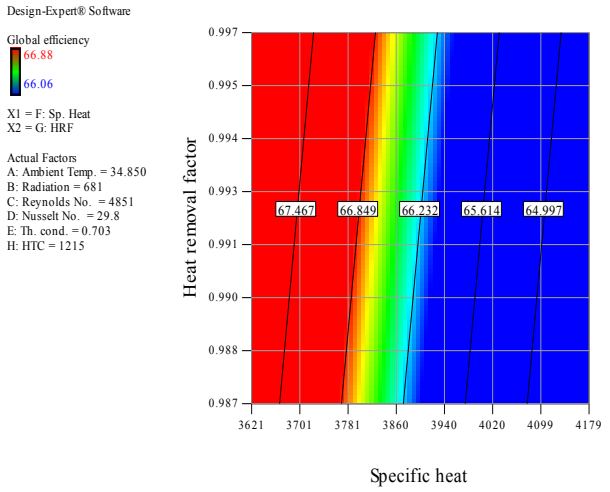

Fig. 7 Variations of specific heat and heat removal factor on η_g

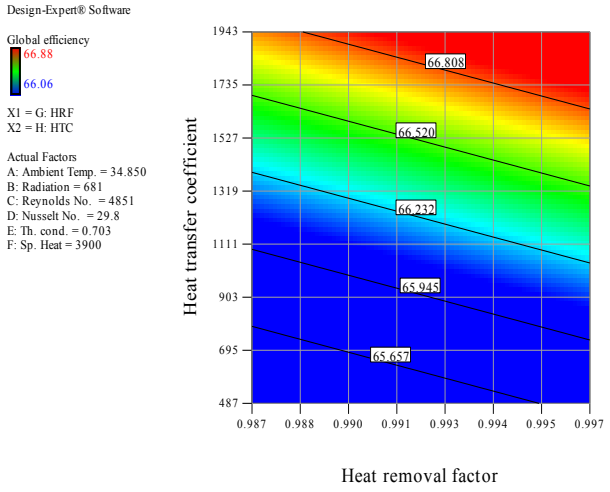

Fig. 8 Variations of heat removal factor and heat transfer coefficient on η_g

After discussing the influencing factors and level of influence over global efficiency, it is important to validate the mathematical correlations derived from the RSM technique, which is used to ensure the equation's consistency and reliability. So, the validation is carried out on a mathematical model to arrive at the difference between the experimental and analytical quantities. Table 3 shows the all input factors, comparison of experimental and analytical results of global efficiency for the whole test duration to understand the deviation. At 1.0% concentration and 0.05 kg/s mass flow rate, it shows the maximum deviation in global efficiency as 0.3520%, but the minimum occurs at 0.5% concentration and 0.02 kg/s mass flow rate.

The maximum deviation occurs for both the instantaneous efficiency and global efficiency at 1.0% concentration and 0.05 kg/s mass flow rate. At 0% concentration, the maximum and minimum deviations are 0.0657% and 0.0031%. 0.1793% and 0.0120% are the two deviation limits, which occur for 4.0% concentration. The average and maximum deviations are 0.1029% and 0.3520%, which ensures perfect agreement between analytical and experimental results. The maximum and average deviation quantities were very less and well within the limit. Therefore, the objective is extended for optimization.

The model's objective is to cross-check the influencing parameter and to identify the altitude where it reaches an optimum level. The mathematical model developed for the global efficiency, which is the function of influencing parameters (ambient temperature, beam radiation, Re, Nu, thermal conductivity, specific heat, heat removal factor, and heat transfer coefficient), to generate optimum parameter values. The maximum and minimum optimized values are obtained using the SOA of DFA (1.0). The minimum and maximum global efficiencies are 49.7% and 84.9%, as per the SOA technique. It corresponds to the minimum and maximum level of radiation (552.41 and 697.23 W/m²) and specific heat (3808.43 and 3814.68 J/kg K).

4. Conclusions

SOA of RSM numerically investigates the experimental performance on shield free nanofluid based parabolic trough solar collector. This numerical investigation explores the influencing factor, level of influence, validation, and optimization. The hierarchy of influencing parameter is solar radiation, the specific heat of nanofluid, the thermal conductivity of nanofluid and ambient temperature, coming under priority; Reynolds number, Nusselt number, heat removal factor, and heat transfer coefficient are the second phase factors.

- The average deviation and maximum deviation of global efficiency are 0.1029% and 0.3520%, are ensuring excellent agreement between analytical and experimental results.
- Based on the desirability function analysis, the maximum and minimum efficiencies are 49.7% and 84.9%, as per the SOA technique.
- The optimized input factor and response values are obtained as follows: ambient temperature (36.803°C), solar radiation (697.23 W/m²), Reynolds number (546.37), Nusselt number (47.75), thermal conductivity of nanofluid (0.6431 W/m·K), specific heat of nanofluid (3814.68 J/kg·K), heat removal factor (0.9964) heat transfer coefficient (1224.23 W/m²K) and global efficiency (84.90) respectively.

Finally, the proposed numerical model suggests enhancing global efficiency by 26.72% by adopting the optimized input parametric quantities.

Nomenclature

A	T_a	Ambient temperature	[°C]
A_c		Aperture area	[m²]
Al_2O_3		Alumina/aluminum oxide	
ANOVA		Analysis of variance	
B	G_b	Beam radiation	[W/m²]
C	Re	Reynolds number	[-]

D	Nu	Nusselt number	[-]
DASC		Direct absorption solar collector	
DFA		Desirability function approach	
E	K	Thermal conductivity	[W/mK]
F	C_P	Specific heat	[J/kgK]
G	F_R	Heat removal factor	[-]
GA		Generic algorithm	
H,	h_f	Heat transfer coefficient	[W/m²K]
HTF		Heat transfer fluid	
PSO		Particle swarm optimization	
PTSC		Parabolic trough solar collector	
R^2		Coefficient of determination	
RSM		Response surface methodology	
SOA		Single objective analysis	
T_i		HTF inlet temperature	[°C]
T_o		HTF outlet temperature	[°C]
T_{Sun}		Sun's surface temperature	[°C]

Greek symbols

ɱ	Nanofluid flow rate,	[kg/s]
ϕ	Volume fraction/concentration	[%]
η	Efficiency	[%]

Subscripts

g	Global
i	Inlet
o	Outlet

References

Alireza, A. (2016). Optimization of solar and wind energy systems: A survey. *International Journal of Ambient Energy,* doi: 10.1080/01430750.2016.1155493.

Amin, R., &Mehran, A. (2020). A comparative study of different optimized mirrors layouts of linear fresnel concentrators on annual energy and exergy efficiencies. *International Journal of Ambient Energy,* doi: 10.1080/01430750.2020.1758780.

Anissa, G., Hatem, M., &Philippe, B. (2015). Numerical study and optimization of parabolic trough solar collector receiver tube. *Journal of Solar Energy Engineering-ASME,* 137, A051003-1; doi:10.1115/1.4030849.

ASHRAE Standard 93-2010, ASHRAE (2010), Atlanta (GA).

Bruno, D., Antonio, J., &Joao F. (2014). Optimization of a seasonal storage solar system using Genetic Algorithms. Solar Energy, 101, 160-166; doi: 10.1016/j.solener.2013.12.031.

Cabello, JM., Cejudo, JM., Luque, M., Ruiz, F., Deb, K., &Tewari, R. (2011). Optimization of the size of a solar thermal electricity plant by means of genetic algorithms. *Renewable Energy*, 36 (11), 3146-3153; doi: 10.1016/j.renene.2011.03.018.

Cheng, ZD., He, YL., Cui, FQ., Du, BC., Zheng, ZJ., &Xu, Y. (2014). Comparative and sensitive analysis for parabolic trough solar collectors with a detailed Monte Carlo ray tracing optical model. *Applied Energy,* 115, 559-572; doi: 10.1016/j.apenergy.2013.11.001.

Cheng, ZD., He, YL., Xiao, J., Tao, YB., & Xu, J. (2010). Three dimensional numerical study of heat transfer characteristics in the receiver tube of parabolic trough solar collector. *International Communications in Heat Transfer,* 37, 782-787; doi: 10.1016/j.icheatmasstransfer.2010.05.002.

Dudley, VE., Kolb, GL., Mahoney, AR., Mancini, TR., Matthews, CW., Sloan, M., &Kearney, D. (1994). Test results: SEGS LS-2 Solar collector, Sandia National Laboratories, Albuquerque, USA, 139; 10.2172/70756.

Farshad, SA., &Sheikholeslami, M. (2019). Simulation of nanoparticles second law treatment inside a solar collector considering turbulent flow. *Physica A:Statistical Mechanics and its Applications,* 525, 1-12; doi: 10.1016/j.physa.2019.03.089.

Hatami, M., & Jing, D. (2017). Optimization of wavy direct absorber solar collector (WDASC) using Al_2O_3-water nanofluid and RSM analysis. *Applied Thermal Engineering,* 121, 1040-1050. doi:10.1016/j.applthermaleng.2017.04.137.

Jiangfeng, G., &Xiulan, H., (2016). Multi-parameter optimization design of parabolic trough solar receiver. *Applied Energy,* 98, 73-79; doi: 10.1016/j.applthermaleng.2015.12.041.

Kline, S., &Mcclintock, F. (1953). Describing uncertainties in single-sample experiments. *Mechanical Engineering*, 75(1), 3-8.

Majedul, I., Azharul, K., Suvash., Saha., Sarah, M., Prasad, KD., &Yarlagadda, V. (2012). Three dimensional simulation of a parabolic trough concentrator thermal collector.In Proceeding of 50th Annual Conference-Australian Solar Energy Society, Melbourne, 1-12.

Moffat, RJ. (1988). Describing the uncertainties in experimental results. Experimental Thermal and Fluid science, 1(1), 3-17; doi: 10.1016/0894-1777(88)90043-X.

Mohamed, A. (2014). Two dimension numerical modelling of receiver tube performance for concentrated solar power plant. *Energy Procedia,* 57, 551-560; doi: 10.1016/j.egypro.2014.10.209.

Mohsen, M., &Mostafa, ZM. (2018). Neural network modeling for accurate prediction of thermal efficiency of a flat plate solar collector working with nanofluids. *International Journal of Ambient Energy,* doi: 10.1080/01430750.2018.1525576.

Moradikazerouni, A., Hajizadeh, A., Safaei, MR., Afrand, M., Yarmand, H., &Zulkifli, NWBM. (2019). Assessment of thermal conductivity enhancement of nano-antifreeze containing single-walled carbon nanotubes: Optimal artificial neural network and curve-fitting. *Physica A: Statistical Mechanics and its Applications,* 521, 138-145; doi: 10.1016/j.physa.2019.01.051.

Petela, R. (2004). Exergy of undiluted thermal radiation, *Solar Energy* 74, 469-488; doi: 10.1016/S0038-092X(03)00226-3.

Rahmati, A., &Niazi, S. (2015). Application and comparison of different lattice Boltzmann methods on non-uniform meshes for simulation of micro cavity and micro channel flow. *Journal of Computational Methods in Engineering,* 34(1), 97-118.

Reza, A., Ehsanolah, A., Rahim, M., Martin, O., Mojtaba, N., & Farzad, P. (2019). Optimization of combined cooling, heating and power (CCHP) systems incorporating the solar and geothermal energy: a review study. *International Journal of Ambient Energy,* doi: 10.1080/01430750.2019.1630299.

Risi., MM., &Laforgia, D. (2013). Modelling and optimization of transparent parabolic trough collector based on gas-phase nanofluids. *Renewable Energy,* 58, 134-139; doi: 10.1016/j.physa.2019.122146.

Saman, R., Masoud, B., Nader, R., &Javad AE. (2017). Steps optimization and productivity enhancement in a nanofluid cascade solar still. *Renewable Energy,* 118, 536-545; doi: 10.1016/j.renene.2017.11.048.

Sami, S. (2018). Impact of magnetic field on the enhancement of performance of thermal solar collectors using nanofluids. *International Journal of Ambient Energy,* doi: 10.1080/01430750.2018.1437561.

Sarafraz, MM., Tlili, I., Zhe, T., Mohsen, B., & Mohammad, RS. (2019). Smart optimization of a thermosyphon heat pipe for an evacuated tube solar collector using response surface methodology (RSM). *Physica A : Statistical Mechanics and its Applications,* 534, 122-146; doi:10.1016/j.physa.2019.122146.

Senthil, R. (2019). Thermal performance of aluminum oxide based nanofluids in flat plate solar collector. *International Journal of Engineering and Advanced Technology,* 8(3), 445-448.

Senthil, R., &Cheralathan, M. (2016). Enhancement of heat absorption rate of direct absorption solar collector using graphite nanofluid, *International Journal of Chemtech Research,* 9(9), 303-308.

Senthil, R., & Cheralathan, M. (2019). Enhancement of the thermal energy storage capacity of a parabolic dish concentrated solar receiver using phase change materials. *Journal of Energy Storage,* 25(100841); doi: 10.1016/j.est.2019.100841.

Shrikant, C., &Guniram, R. (2018). Thermodynamic investigation of nano-phase change materials as heat transfer fluid- heat exchanger for thermal-energy storage in concentrating solar thermo-electric generation systems. *Journal of Ambient Energy,* doi: 10.1080/01430750.2018.1517691.

Tahereh, BG., & Ranjbar, AA. (2015). Geometric optimization of a nanofluid-based direct absorption solar collector using response surface methodology. *Solar Energy,* 122, 314-325; doi: 10.1016/j.solener.2015.09.007.

Tahereh, BG., &Ranjbar, AA. (2017). Thermal and exergy optimization of a nanofluid-based direct absorption solar collector. *Renewable Energy,*106, 274-287; doi: 10.1016/j.renene.2017.01.031.

Venkata Rao, R., &Hameer Singh, Keesari. (2019). Solar assisted heat engine systems: multi objective optimization and decision making. *International Journal of Ambient Energy,* doi: 10.1080/01430750.2019.1636870.

Vijayan, G., &Karunakaran, R. (2019). Performance evaluation of nanofluid on parabolic trough solar collector. *Thermal Science,* 24(2A), 853-864; doi: 10.2298/TSCI180509059G.

Vijayan, G., Karunakaran, R., Logesh, K., Sivasaravanan, S., &Metin, Kok. (2019). Influence of dimensionless parameter on deionized water-alumina nanofluid based parabolic trough solar collector. *Recent Patents on Nanotechnology,* 13(3), 206-221; doi: 10.2174/1872210513666190410123503.

Ze-Dong, C., Ya-Ling, H., Bao-Cun, D., Kun, W., &Qi, L. (2015). Geometric optimization on optical performance of parabolic trough solar collector systems using particle swarm optimization algorithm. *Applied Energy,* 148, 282-293; doi: 10.1016/j.apenergy.2015.03.079.